Biochim Biophys Acta, 1864:894-899 (2017)

Formatted: Wrap Around
Field Code Changed

Measuring Ca^{2+} inside intracellular organelles with luminescent and fluorescent aequorin-based sensors

María Teresa Alonso, Jonathan Rojo-Ruiz, Paloma Navas-Navarro, Macarena Rodríguez-Prados and Javier García-Sancho

Instituto de Biología y Genética Molecular (IBGM), Universidad de Valladolid and Consejo Superior de Investigaciones Científicas (CSIC), c/ Sanz y Forés 3, 47003 Valladolid, Spain

Corresponding authors: Javier García-Sancho (jgsancho@ibgm.uva.es) or María Teresa Alonso (talonso@ibgm.uva.es), IBGM, c/ Sanz y Forés 3, 47003 Valladolid, Spain. Fax: +34-983-184800; Phone: +34-983-423085.

Special issue with BBA-Molecular Cell Research**. ECS meeting**, Guest Editors: Jacques Haiech, Claus Heizmann and Joachim Krebs

Abbreviations: GAP, GFP-Aequorin Protein; ER, endoplasmic reticulum; SR, sarcoplasmic reticulum; SERCA, sarco-endoplasmic reticulum Ca^{2+} ATPase; TBH, tert-butyl-hidroquinone; GECI, genetically encoded calcium indicator; GFP, green fluorescent protein; $[Ca^{2+}]_C$, $[Ca^{2+}]_{ER}$, $[Ca^{2+}]_{SR}$, $[Ca^{2+}]_{GO}$, Ca^{2+} concentrations in cytosol, ER, SR or Golgi apparatus, respectively. CICR, Ca^{2+}-induced Ca^{2+}-release.

Formatted: Wrap Around

Field Code Changed

ABSTRACT

GFP-Aequorin fusion Proteins (GAP) can be used to measure [Ca^{2+}] inside intracellular organelles, both by luminescence and by fluorescence. The low-affinity variant GAP3 is adequate for ratiometric imaging in the endoplasmic reticulum and Golgi apparatus, and it can be combined with conventional synthetic indicators for simultaneous measurements of cytosolic Ca^{2+}. GAP is biorthogonal as it does not have mammalian homologues, and it is robust and functionally expressed in transgenic flies and mice, where it can be used for Ca^{2+} measurements *ex vivo* and *in vivo* to explore animal models of health and disease.

KEYWORDS: biosensor, calcium, organelles, GFP, aequorin, GECI, endoplasmic reticulum, Golgi apparatus.

Highlights

- GFP-Aequorin fusion proteins (GAP) are a new family of Ca^{2+} sensors.
- They are suitable for ratiometric Ca^{2+} imaging in cytoplasmic organelles.
- Low Ca^{2+} affinity can be engineered for high Ca^{2+} organelles such as ER or Golgi.
- GAPs are bioorthogonal and transgenic animals show normal phenotype.
- *Ex vivo* and *in vivo* measurements are possible in transgenic mice and flies.

Formatted: Wrap Around

Field Code Changed

1. INTRODUCTION

Calcium signalling is the trigger of many biological processes in animal cells [1]. Emphasis was traditionally focused on cytosolic Ca^{2+} ($[Ca^{2+}]_C$), but much attention has been placed in recent years on Ca^{2+} inside intracellular organelles such as nucleus, mitochondria, endoplasmic reticulum (ER) or Golgi apparatus. The luminal Ca^{2+} concentration in the ER ($[Ca^{2+}]_{ER}$) or the Golgi apparatus ($[Ca^{2+}]_{GO}$) is maintained in the 0.2-2 mM range, three orders of magnitude above $[Ca^{2+}]_C$. These high Ca^{2+} concentrations are essential for proper functioning, and disturbances occasion stress and ‘‘unfolded protein response’’ in the ER [2] and defects in protein segregation and cargo sorting in the Golgi apparatus [3].

Although some synthetic Ca^{2+} indicators such as rhod-2, rhod-5N, magfura-2 or magfluo-3 have been used to measure organellar Ca^{2+} content (**Table 1**), the selectivity of these probes is poor, and measurements have many drawbacks [4]. In contrast, genetically encoded calcium indicators (GECI) can be precisely targeted to intraluminal locations within the selected organelle. The photoluminescent protein aequorin, extracted from the jellyfish *Aequorea victoria* [5], was originally injected into cells to follow the $[Ca^{2+}]_C$ transients associated with action potentials [6]. After cloning of its gene, recombinant aequorins were used to monitor Ca^{2+} transients in mitochondria [7], ER, Golgi or secretory vesicles [8]. Aequorins are useful, clean and reliable probes to follow Ca^{2+} signals, although its light output is poor and this makes imaging difficult [9].

Fluorescent GECIs show stronger light output than bioluminescent probes and, therefore, are more suitable for Ca^{2+} imaging. They are classified into two main families: those composed of two fluorescent proteins, such as the cameleons; and the ones based on a single fluorescent protein, such as the GCaMs. The Ca^{2+}-binding sites are provided by the endogenous proteins calmodulin (CaM) or troponin C (TnC).

Formatted: Wrap Around

Field Code Changed

Cameleons consist of CaM fused to a short CaM-binding peptide (M13), flanked by two fluorescent proteins. The binding of Ca^{2+} to CaM or TnC increases Förster resonance energy transfer (FRET), leading to a change in the signal, with increased fluorescence at the longer wavelength and decreased fluorescence at the shorter one.

The second class of indicators consists of a single fluorescent protein, often circularly permuted (cp), fused to an N-terminal M13 peptide and a C-terminal CaM domain. The Ca^{2+}-dependent interaction of CaM with M13 modifies the environment of the chromophore in the fluorescent protein in such a way that the signal increases. Two GCaM derivative families include the variants of distinct cues, GECOs [10] and low-affinity CEPIAs [11]. The CatchER family of indicators consists of a single EF-hand motif inserted in GFP [12]. A selection of the low affinity GECIs with their main characteristics are listed in **Table 1**. Previous reviews focused on different aspects of GECIS ([13, 14]. Here we shall center on the development and applications of a new class of low affinity Ca^{2+} indicators containing aequorin fused to GFP (GFP-Aequorin Protein, GAP), or other fluorescencent proteins, and which can be used either as luminescent or fluorescent Ca^{2+} sensors.

Formatted: Wrap Around

Field Code Changed

2. RESULTS AND DISCUSSION

2.1. Modified aequorins

Besides the wild type aequorin, which emits blue luminescence in the presence of Ca^{2+} and the cofactor coelenterazine, modified aequorins emitting at different wavelenths have been generated by fusion to different fluorescent proteins, green (GFP), red (mRFP) or tandem dimer tomato (tDT) [15-18]. Red aequorins provide the advantage that emission can be detected across the skin and other tissues, permitting *in vivo* measurements [18]. In addition , targeting of red and green aequorins to different subcellular compartments enables simultaneous monitoring of Ca^{2+} levels in two organelles [17].

Further useful modifications of aequorins include engineering for optimizing its affinity for Ca^{2+} to the Ca^{2+} concentration range found in the organelles to be measured. For example, the Ca^{2+} concentration expected in the lumen of the ER or the Golgi apparatus ranges from 0.2 to 2 mM. The higher Ca^{2+} concentrations would provoke a complete consumption of the aequorin with cessation of luminescence in a few seconds [19]. Hence, several substitutions in the EF hands of the aequorin have been introduced in order to reduce the affinity for Ca^{2+}. In addition, various modified coelenterazines can also be used to modify the Ca^{2+} affinity [20].

Aequorins with different Ca^{2+} affinities are compared in **Figure 1A**. The wild type aequorin (named 1 in **Figure 1A**) enables measurements at around 10^{-6} M [Ca^{2+}], but at 5 µM the rate of consumption would be about 1 % per second, leading to consumption of most of the aequorin within a few minutes. Wild type aequorin in conjunction with coelenterazine n (2 in the **Figure 1A**) allows accurate [Ca^{2+}] quantification within the 2-20 µM range, and can be applied to measure moderate Ca^{2+}

Formatted: Wrap Around

Field Code Changed

overloads in the mitochondria [21]. Measuring [Ca^{2+}] in the lumen of the ER was first achieved by combining a D119A (aspartic acid in position 119 exchanged by alanine) substitution in apoaequorin together with coelenterazine n [22]. This mixture (3 in **Figure 1A**) gives reliable estimations in the 20-1000 µM range, and is suitable for measurements in the ER, the Golgi apparatus and the overloaded mitochondria [21-23]. The fusion of the mutated aequorin to GFP (GFP-aequorin, mutGA in **Figure 1A**) produced minor effects on the affinity for Ca^{2+}[17].

The classical low affinity aequorin system (3 and ermutGA in **Figure 1A**) gets quickly consumed at high Ca^{2+} levels (near 1% per second at 10^{-3} M), and that prevents accurate measurements during experiments lasting for more than a few minutes. At 37 ºC the problem is even worse as consumption is accelerated further (1b in **Figure 1A**). In order to overcome these limitations, two extra-low affinity aequorins have been recently developed. The new indicator GAP1 is a GFP-Aequorin Protein fusion (GAP, see below), where three substitutions, D117A, D119A and D163A, have been introduced in the aequorin moiety. Combining this indicator with coelenterazine n allows comfortable measurements in the 100-2000 µM range [24] (GAP1 in **Figure 1A**). Even lower affinity is achieved by the double mutated D119A and N28L aequorin reconstituted with coelenterazine i (er2mutA in **Figure 1A**) [25], that increases the range of [Ca^{2+}] measurements up to 10 mM. The use of this extra low affinity aequorin sometimes permits detection of ER subcompartmets with Ca^{2+} concentrations as high as 2 mM, which cannot be detected with other systems because of rapid burning of the aequorin [25].

2.2. GAP, a new family of fluorescent Ca^{2+} sensors for intracellular organelles

We realized recently that some of the GFP-Aequorin fusion Proteins (GAP) we developed for bioluminescence measurements also exhibited a Ca^{2+}-dependent

Formatted: Wrap Around

Field Code Changed

fluorescence, with changes in the excitation spectrum of the green fluorescence. Coelenterazine was not required indicating that the phenomenon is due to the interaction between the two moieties, GFP and aequorin, and that it is not related to the luminescence reaction [26]. Upon Ca^{2+} binding, the fluorescence excited at 470 nm increases with a parallel decrease of the fluorescence excited at 405 nm. This enables ratiometric measurements that provide a more reliable quantificatation and are less prone to imaging artifacts. In addition, GAP indicators can be used in combination with synthetic probes such as fura or rhod dyes for simultaneous cytosolic and intraorganelle Ca^{2+} measurements.

The dynamic range of GAP, determined as the maximum change in the F_{470}/F_{405} ratio, is 3-4. The Ca^{2+} calibration curve follows the Hill function, $y/y_{max} = [Ca^{2+}]^n / (K_D^n + [Ca^{2+}]^n)$, where $y = (R-R_{min})/(R_{max}-R_{min})$and the Hill coefficient (n) is 1 (**Figure 1B**). This makes the calibration easier and increases the useful concentration range of the probe (more than one order of magnitude for R values from 0.2 to 0.8). The K_D for Ca^{2+} is 0.2 µM, suitable for measurements of $[Ca^{2+}]_C$, and it can be modified by genetic engineering of the three aequorin EF hands (see below). Importantly, this indicator is insensitive to Mg^{2+} in the 0.1-5 mM range and to H^+ in the 6.5-8.5 pH range. The probe was successfully targeted to cytosol (excluding the intracellular organelles), nucleus, mitochondria, ER or Golgi apparatus [26]. In contrast to most of the GECIS, which are based in calmodulin or troponin, the Ca^{2+}-responsive element of GAP is the photoprotein apoaequorin [26]. This makes of GAP a unique dual calcium sensor, able to function either as a fluorescent or as a bioluminescent indicator (**Figure1C**).

GFP and aequorin, the two proteins from *Aequorea Victoria* in which GAP is based, do not have mammalian homologues. As a consequence, the possibility of interaction between GAP and endogenous partners is minimized, and this makes GAP a truly orthogonal calcium indicator, in contrast to other indicators with calcium-binding

Formatted: Wrap Around

Field Code Changed

elements coming from animal proteins. Consistently, transgenic mice expressing GAP ubiquitously were viable and did not show phenotypic anomalies, even though expression was specially prominent in neural tissues [26].

2.3. Low affinity GAPs

As mentioned above, adequate affinity of the indicator is essential for accurate measurement in the selected organellar environment. Thereupon, much effort was dedicated to generate low affinity GAPs that conform to the high [Ca^{2+}]-organelles (**Figure 1B**). The first successful derivative, named GAP1, displayed a K_D of 17 µM and preserved all the other beneficial properties of the original GAP. It would be very adequate for measurements in mitochondria at submaximal Ca^{2+} overloads or in one of the subcompartments of trans-Golgi network with $[Ca^{2+}]_{GO}$= 50 µM [23]. However, the affinity is too high for reliable measurements in the ER lumen, where [Ca^{2+}] approaches 1 mM. Consistently, although GAP1 is able to detect large decreases in the ER Ca^{2+} effected by massive Ca^{2+} release, it was not sensitieve enough to detect moderate fluctuations in the ER Ca^{2+} content [26]. Further optimization of GAP for use in ER led to GAP2, that contains the mutations D119A and D24N, and has a K_D for Ca^{2+} of 400-500 µM (**Figure 1B**). This affinity is optimal for measurements in the ER, where [Ca^{2+}] values of 200-1000 µM have been reported [27-30]. Finally, we prepared GAP3, a GAP2 derivative with the same affinity and optimized for expression in mammalian cells. GAP3 should be generally chosen for measurements in the ER or the Golgi apparatus (**Figure 1B**) [31].

2.4. GAP3 is optimal for monitoring $[Ca^{2+}]_{ER}$ and $[Ca^{2+}]_{GO}$

We have recently described functional results obtained in model cell lines and in primary cultures of cells expressing GAP3 in the ER [31]. The indicator successfully

Formatted: Wrap Around

Field Code Changed

reported $[Ca^{2+}]_{ER}$ dynamics and was sensitive enough to follow luminal Ca^{2+} oscillations inside the ER of astrocytes. Moreover, we have generated transgenic animals (mice and flies) expressing ER-targeted GAP3 (erGAP3). No phenotypic alterations were detected in these animals, which were used to provide the proofs of concept for the suitability of the probe to monitor $[Ca^{2+}]_{ER}$ under conditions close to the physiological ones. For example, we performed a functional mapping of acetylcholine receptors in acute isolated hippocampal slices by studying the agonist-induced Ca^{2+} release from the ER through direct monitoring changes of $[Ca^{2+}]_{ER}$ (**Figure 2A**). We found that only the CA1 region responded to acetylcholine with Ca^{2+} release from the ER, in agreement with the reported expression of the muscarinic acetylcholine receptors in this area [32, 33]. Mapping of ER release with other agonists resulted in different maps (results not show).

We simultaneously imaged the ER- and the cytosolic-Ca^{2+} dynamics using the erGAP3 (**Figure 2A**) and rhod-3 signals, respectively. Interestingly, we found that the $[Ca^{2+}]_C$ peak preceded maximal ER release. This result evidences the continuous clearance of the cytosolic Ca^{2+} by homeostatic mechanisms. We have shown in chromaffin cells that the relative contribution of different mechanism to the cytosolic Ca^{2+} clearance depends on $[Ca^{2+}]_C$ [29]. At low $[Ca^{2+}]_C$ the high affinity Ca^{2+} pumps, the sarco-endoplasmic reticulum Ca^{2+} ATPase (SERCA) and the plasma membrane Ca^{2+}-ATPase (PMCA), predominate. On the contrary, at higher $[Ca^{2+}]_C$ the low-affinity mitochondrial Ca^{2+} uniporter predominates, and Ca^{2+} is taken up into mitochondria. If the rate of mitochondrial uptake exceeds ER exit then $[Ca^{2+}]_C$ decreases, as seen here. Note that $[Ca^{2+}]_C$ at the ER-mitochondria junction microdomains may very much exceed the mean $[Ca^{2+}]_C$ reported by the cytosolic Ca^{2+} probe.

In order to demonstrate the feasibility of *in vivo* measurements with the new Ca^{2+} sensors, we genetically engineered *Drosophila* to express erGAP3 specifically in the

Formatted: Wrap Around

Field Code Changed

sarcoplasmic reticulum of striated muscles and then recorded the fluorescence signal in the easily accessible thoracic muscles [31]. These muscles may be conveniently stimulated in the living fly through the giant fiber system, which activates all the motor neurones simultaneously [34]. **Figure 3** illustrates the results of one of such experiments in which stimulation was performed at different frequencies (from 0.25 up to 16 Hz), and fluorescence images were collected every 100 ms. At the lowest frequency (0.25 Hz) the unitary release events, with sudden decrease of $[Ca^{2+}]_{ER}$, can be perfectly distinguished every 4 s (**Figure 3A**). Release was very fast, as the decrease of $[Ca^{2+}]_{ER}$ had been completed within 100 ms, and was followed by a slower reuptake, with $t_{1/2}$ close to 1 s. At higher frequencies (4 and 16 Hz) the individual release events fused together leading to a larger $[Ca^{2+}]_{ER}$ drop. $[Ca^{2+}]_{ER}$ decreased during the first 1-1.5 s and then the ER began to refill even though the electric stimulation continued for 4 s. This decrease of $[Ca^{2+}]_{ER}$ release may be due to synaptic fatigue at the neuromuscular junction. When the electric stimulation ceased the rate of sarcoplasmic reticulum refilling increased (**Figure 3A**). **Figure 3B** shows pseudo-color coded GAP3 fluorescence images of the fly thorax normalized as R/R_0. Note that the decrease in fluorescence was homogeneous in all the thorax muscles.

In **Figure 3C** the time courses of $[Ca^{2+}]_{ER}$ during stimulation at the three different frequencies has been superimposed for comparing amplitudes and rates. Note that prior to fatigue the elementary events tend to have the same amplitude, about 0.01 scale units. The initial rate of $[Ca^{2+}]_{ER}$ decrease is also similar in all the cases. In the case of stimulation at 4 Hz (1 stimulus each 0.25 s *vs* sampling at 1 image every 0.10 s) the expected saw-tooth-like aspect was observed due to alternation between decrease and increase of the fluorescence signal in two consecutive time points.

In **conclusion**, we review here a new family of Ca^{2+} probes named GAP, that are GFP-Aequorin fusion Proteins. They can be used either as luminescent or as fluorescent

Formatted: Wrap Around

Field Code Changed

probes and can be targeted to cytoplasmic organelles. The low Ca^{2+} affinity variants, adequate for measurements in high-Ca^{2+} environments such as the ER or the Golgi apparatus, are particularly addressed to. In the luminescent mode GAP allows to perform long term measurements (up to 1 hour) in minimally perturbed tissues. In fluorescence mode GAP permits ratiometric measurements and imaging, and it can be combined with conventional synthetic indicators for simultaneous measurements of the cytosolic Ca^{2+}. Calibration of GAP is uncomplicated as the Hill coefficient is 1. As the building blocks of GAP do not have mammalian homologues, no interferences with endogenous proteins should be expected, so that the sensor is, in contrast to other precedent indicators, bioorthogonal. Transgenic flies and mice, with robust functional expression in different areas including the central nervous system, show a normal phenotype and can be used for Ca^{2+} measurements *ex vivo* and *in vivo.*

Formatted: Wrap Around

Field Code Changed

ACKNOWLEDGMENTS

This work was supported by grants from the Spanish Ministerio de Economia y Competitividad (BFU2014-53469P) and the Instituto de Salud Carlos III (TerCel; RD16/0011/0003), and co-financed by the European Union through the European Regional Development Fund.

Formatted: Wrap Around

Field Code Changed

REFERENCES

[1] D.E. Clapham, Calcium signaling, Cell, 131 (2007) 1047-1058.

[2] S. Gallego-Sandin, M.T. Alonso, J. Garcia-Sancho, Calcium homoeostasis modulator 1 (CALHM1) reduces the calcium content of the endoplasmic reticulum (ER) and triggers ER stress, Biochem J, 437 (2011) 469-475.

[3] C. Kienzle, J. von Blume, Secretory cargo sorting at the trans-Golgi network, Trends Cell Biol, 24 (2014) 584-593.

[4] R.I. Fonteriz, S. de la Fuente, A. Moreno, C.D. Lobaton, M. Montero, J. Alvarez, Monitoring mitochondrial [Ca(2+)] dynamics with rhod-2, ratiometric pericam and aequorin, Cell Calcium, 48 (2010) 61-69.

[5] O. Shimomura, A short story of aequorin, Biol Bull, 189 (1995) 1-5.

[6] R. Llinas, J.R. Blinks, C. Nicholson, Calcium transient in presynaptic terminal of squid giant synapse: detection with aequorin, Science, 176 (1972) 1127-1129.

[7] R. Rizzuto, A.W. Simpson, M. Brini, T. Pozzan, Rapid changes of mitochondrial Ca2+ revealed by specifically targeted recombinant aequorin, Nature, 358 (1992) 325-327.

[8] V. Granatiero, M. Patron, A. Tosatto, G. Merli, R. Rizzuto, Using targeted variants of aequorin to measure Ca2+ levels in intracellular organelles, Cold Spring Harb Protoc, 2014 (2014) 86-93.

[9] C. Villalobos, L. Nunez, P. Chamero, M.T. Alonso, J. Garcia-Sancho, Mitochondrial [Ca(2+)] oscillations driven by local high [Ca(2+)] domains generated by spontaneous electric activity, J Biol Chem, 276 (2001) 40293-40297.

Formatted: Wrap Around

Field Code Changed

[10] Y. Yamada, K. Mikoshiba, Quantitative comparison of novel GCaMP-type genetically encoded Ca(2+) indicators in mammalian neurons, Front Cell Neurosci, 6 (2012) 41.

[11] J. Suzuki, K. Kanemaru, K. Ishii, M. Ohkura, Y. Okubo, M. Iino, Imaging intraorganellar Ca2+ at subcellular resolution using CEPIA, Nat Commun, 5 (2014) 4153.

[12] J. Wu, D.L. Prole, Y. Shen, Z. Lin, A. Gnanasekaran, Y. Liu, L. Chen, H. Zhou, S.R. Chen, Y.M. Usachev, C.W. Taylor, R.E. Campbell, Red fluorescent genetically encoded Ca2+ indicators for use in mitochondria and endoplasmic reticulum, Biochem J, 464 (2014) 13-22.

[13] J. Suzuki, K. Kanemaru, M. Iino, Genetically Encoded Fluorescent Indicators for Organellar Calcium Imaging, Biophys J, 111 (2016) 1119-1131.

[14] Y. Zhao, S. Araki, J. Wu, T. Teramoto, Y.F. Chang, M. Nakano, A.S. Abdelfattah, M. Fujiwara, T. Ishihara, T. Nagai, R.E. Campbell, An expanded palette of genetically encoded Ca(2)(+) indicators, Science, 333 (2011) 1888-1891.

[15] V. Baubet, H. Le Mouellic, A.K. Campbell, E. Lucas-Meunier, P. Fossier, P. Brulet, Chimeric green fluorescent protein-aequorin as bioluminescent Ca2+ reporters at the single-cell level, Proc Natl Acad Sci U S A, 97 (2000) 7260-7265.

[16] T. Curie, K.L. Rogers, C. Colasante, P. Brulet, Red-shifted aequorin-based bioluminescent reporters for in vivo imaging of Ca2 signaling, Mol Imaging, 6 (2007) 30-42.

Formatted: Wrap Around

Field Code Changed

[17] I.M. Manjarres, P. Chamero, B. Domingo, F. Molina, J. Llopis, M.T. Alonso, J. Garcia-Sancho, Red and green aequorins for simultaneous monitoring of Ca2+ signals from two different organelles, Pflugers Arch, 455 (2008) 961-970.

[18] A. Bakayan, B. Domingo, A. Miyawaki, J. Llopis, Imaging Ca(2+) activity in mammalian cells and zebrafish with a novel red-emitting aequorin variant, Pflugers Arch, 467 (2015) 2031-2042.

[19] M.T. Alonso, C. Villalobos, P. Chamero, J. Alvarez, J. Garcia-Sancho, Calcium microdomains in mitochondria and nucleus, Cell Calcium, 40 (2006) 513-525.

[20] O. Shimomura, B. Musicki, Y. Kishi, S. Inouye, Light-emitting properties of recombinant semi-synthetic aequorins and recombinant fluorescein-conjugated aequorin for measuring cellular calcium, Cell Calcium, 14 (1993) 373-378.

[21] M. Montero, M.T. Alonso, E. Carnicero, I. Cuchillo-Ibanez, A. Albillos, A.G. Garcia, J. Garcia-Sancho, J. Alvarez, Chromaffin-cell stimulation triggers fast millimolar mitochondrial Ca2+ transients that modulate secretion, Nat Cell Biol, 2 (2000) 57-61.

[22] M.J. Barrero, M. Montero, J. Alvarez, Dynamics of [Ca2+] in the endoplasmic reticulum and cytoplasm of intact HeLa cells. A comparative study, J Biol Chem, 272 (1997) 27694-27699.

[23] F.J. Aulestia, M.T. Alonso, J. Garcia-Sancho, Differential calcium handling by the cis and trans regions of the Golgi apparatus, Biochem J, 466 (2015) 455-465.

Formatted: Wrap Around

Field Code Changed

[24] M. Rodriguez-Prados, J. Rojo-Ruiz, F.J. Aulestia, J. Garcia-Sancho, M.T. Alonso, A new low-Ca(2)(+) affinity GAP indicator to monitor high Ca(2)(+) in organelles by luminescence, Cell Calcium, 58 (2015) 558-564.

[25] S. de la Fuente, R.I. Fonteriz, M. Montero, J. Alvarez, Ca2+ homeostasis in the endoplasmic reticulum measured with a new low-Ca2+-affinity targeted aequorin, Cell Calcium, 54 (2013) 37-45.

[26] A. Rodriguez-Garcia, J. Rojo-Ruiz, P. Navas-Navarro, F.J. Aulestia, S. Gallego-Sandin, J. Garcia-Sancho, M.T. Alonso, GAP, an aequorin-based fluorescent indicator for imaging Ca2+ in organelles, Proc Natl Acad Sci U S A, 111 (2014) 2584-2589.

[27] M.T. Alonso, M.J. Barrero, E. Carnicero, M. Montero, J. Garcia-Sancho, J. Alvarez, Functional measurements of [Ca2+] in the endoplasmic reticulum using a herpes virus to deliver targeted aequorin, Cell Calcium, 24 (1998) 87-96.

[28] J. Alvarez, M. Montero, Measuring [Ca2+] in the endoplasmic reticulum with aequorin, Cell Calcium, 32 (2002) 251-260.

[29] C. Villalobos, L. Nunez, M. Montero, A.G. Garcia, M.T. Alonso, P. Chamero, J. Alvarez, J. Garcia-Sancho, Redistribution of Ca2+ among cytosol and organella during stimulation of bovine chromaffin cells, FASEB J, 16 (2002) 343-353.

[30] M.T. Alonso, M.J. Barrero, P. Michelena, E. Carnicero, I. Cuchillo, A.G. Garcia, J. Garcia-Sancho, M. Montero, J. Alvarez, Ca2+-induced Ca2+ release in chromaffin cells seen from inside the ER with targeted aequorin, J Cell Biol, 144 (1999) 241-254.

Formatted: Wrap Around

Field Code Changed

[31] P. Navas-Navarro, J. Rojo-Ruiz, M. Rodriguez-Prados, M.D. Ganfornina, L.L. Looger, M.T. Alonso, J. Garcia-Sancho, GFP-Aequorin Protein Sensor for Ex Vivo and In Vivo Imaging of Ca(2+) Dynamics in High-Ca(2+) Organelles, Cell Chem Biol, 23 (2016) 738-745.

[32] D. Fernandez de Sevilla, A. Nunez, M. Borde, R. Malinow, W. Buno, Cholinergic-mediated IP3-receptor activation induces long-lasting synaptic enhancement in CA1 pyramidal neurons, J Neurosci, 28 (2008) 1469-1478.

[33] J.M. Power, P. Sah, Nuclear calcium signaling evoked by cholinergic stimulation in hippocampal CA1 pyramidal neurons, J Neurosci, 22 (2002) 3454-3462.

[34] M.J. Allen, T.A. Godenschwege, Electrophysiological recordings from the Drosophila giant fiber system (GFS), Cold Spring Harb Protoc, 2010 (2010) pdb prot5453.

[35] A.M. Hofer, T.E. Machen, Technique for in situ measurement of calcium in intracellular inositol 1,4,5-trisphosphate-sensitive stores using the fluorescent indicator mag-fura-2, Proc Natl Acad Sci U S A, 90 (1993) 2598-2602.

[36] F.A. Lattanzio, Jr., D.K. Bartschat, The effect of pH on rate constants, ion selectivity and thermodynamic properties of fluorescent calcium and magnesium indicators, Biochem Biophys Res Commun, 177 (1991) 184-191.

[37] O. Tour, S.R. Adams, R.A. Kerr, R.M. Meijer, T.J. Sejnowski, R.W. Tsien, R.Y. Tsien, Calcium Green FlAsH as a genetically targeted small-molecule calcium indicator, Nat Chem Biol, 3 (2007) 423-431.

Formatted: Wrap Around

Field Code Changed

[38] A. Miyawaki, J. Llopis, R. Heim, J.M. McCaffery, J.A. Adams, M. Ikura, R.Y. Tsien, Fluorescent indicators for Ca2+ based on green fluorescent proteins and calmodulin, Nature, 388 (1997) 882-887.

[39] A.E. Palmer, C. Jin, J.C. Reed, R.Y. Tsien, Bcl-2-mediated alterations in endoplasmic reticulum Ca2+ analyzed with an improved genetically encoded fluorescent sensor, Proc Natl Acad Sci U S A, 101 (2004) 17404-17409.

[40] A.E. Palmer, M. Giacomello, T. Kortemme, S.A. Hires, V. Lev-Ram, D. Baker, R.Y. Tsien, Ca2+ indicators based on computationally redesigned calmodulin-peptide pairs, Chem Biol, 13 (2006) 521-530.

[41] K. Ishii, K. Hirose, M. Iino, Ca2+ shuttling between endoplasmic reticulum and mitochondria underlying Ca2+ oscillations, EMBO Rep, 7 (2006) 390-396.

[42] S. Tang, H.C. Wong, Z.M. Wang, Y. Huang, J. Zou, Y. Zhuo, A. Pennati, G. Gadda, O. Delbono, J.J. Yang, Design and application of a class of sensors to monitor Ca2+ dynamics in high Ca2+ concentration cellular compartments, Proc Natl Acad Sci U S A, (2011).

[43] T. Thestrup, J. Litzlbauer, I. Bartholomaus, M. Mues, L. Russo, H. Dana, Y. Kovalchuk, Y. Liang, G. Kalamakis, Y. Laukat, S. Becker, G. Witte, A. Geiger, T. Allen, L.C. Rome, T.W. Chen, D.S. Kim, O. Garaschuk, C. Griesinger, O. Griesbeck, Optimized ratiometric calcium sensors for functional in vivo imaging of neurons and T lymphocytes, Nat Methods, 11 (2014) 175-182.

[44] M. Waldeck-Weiermair, H. Bischof, S. Blass, A.T. Deak, C. Klec, T. Graier, C. Roller, R. Rost, E. Eroglu, B. Gottschalk, N.A. Hofmann, W.F. Graier, R.

Malli, Generation of Red-Shifted Cameleons for Imaging Ca(2)(+) Dynamics of the Endoplasmic Reticulum, Sensors (Basel), 15 (2015) 13052-13068.

[45] M.J. Henderson, H.A. Baldwin, C.A. Werley, S. Boccardo, L.R. Whitaker, X. Yan, G.T. Holt, E.R. Schreiter, L.L. Looger, A.E. Cohen, D.S. Kim, B.K. Harvey, A Low Affinity GCaMP3 Variant (GCaMPer) for Imaging the Endoplasmic Reticulum Calcium Store, PLoS One, 10 (2015) e0139273.

Formatted: Wrap Around

Field Code Changed

Formatted: Wrap Around

Field Code Changed

FIGURE CAPTIONS

Figure 1. Ca^{2+} calibration of aequorins (A) and GAPs (B).

(A) Except when otherwise stated, all the calibrations are at 22 ºC. **1.** Wild-type (Wt) aequorin (AEQ) with wt-coelenterazine (Cz). **1b.** Same as 1, but at 37 ºC. **2.** Wt-AEQ with Cz n. **3.** ^{D119A}AEQ with Cz n. **ermutGA**, er-targeted GFP-^{D119A}AEQ with Cz n. **GAP1**, GFP-$^{D117A,\ D119A,\ D163A}$AEQ with Cz n. **er2mutAEQ**, ^{N28L,D119A}AEQ with Cz i at 37ºC. Data in ordinate are counts/total counts (s^{-1}). Note double logarithmic scales. Data taken from [17, 21, 22, 24, 25]. **(B)** Calibration of GAPs. Adjusted to $y/y_{max}=([Ca^{2+}]^n) / (K_D^n + [Ca^{2+}]^n)$, where $y = ((R-R_{min})/(R_{max}-R_{min}))$, with n = 1. The values of K_D (µM) were: GAP, 0.2; GAP1, 17; GAP3, 450-500. The affinities of GAP2 and GAP3 were undistinguishable. Data taken from: [26, 31]. (C) Model comparing the action of GAP as luminescent (left) and fluorescent probe (right). Ca^{2+} is the trigger in both cases. For luminescence emission combination of AEQ with the cofactor, Cz, is necessary. In contrast, Cz is not required nor does it modify fluorescence emission. Modified from Rodriguez-Prados et al, 2015.

Figure 2. Functional mapping of ER Ca^{2+} release induced by acethylcholine (ACh) erGAP3 in mice hippocampus.

(A) Frame sequence during stimulation with acetylcholine (ACh; 200 µM, 30 s) in acute hippocampal slices from erGAP3 transgenic mice (line 10; P7). Cornus ammonis regions (CA) and the upper blade of dentate gyrus (DG) are visible. Measurements of ER- (erGAP3) and cytosolic Ca^{2+} (rhod-3) were performed simultaneously. Frames were acquired every 10 s. Upper row: ER Ca^{2+} release, evidenced by the decrease of the GAP signal in CA1, during ACh stimulation. Calibration bar, 200 µm. Lower row,

Formatted: Wrap Around

Field Code Changed

coordinated increase of rhod-3 fluorescence, indicating the increase of $[Ca^{2+}]_C$ by release from the ER. **(B)** Detailed kinetics of experiment shown in **(A)**. Each graph symbol corresponds to 10 s. Note that the peak increase of $[Ca^{2+}]_C$ occurs 10 s after the application of ACh, whereas maximum $[Ca^{2+}]_{ER}$ decrease required more than 30 s. The relaxation of the $[Ca^{2+}]_C$ peak was also faster than the one of the $[Ca^{2+}]_{ER}$ peak. Reproduced with permission from Navas-Navarro *et al.*, 2016

Figure 3. Stimulation of motor neurones promotes Ca^{2+} release from muscle sarcoplasmic reticulum.

Experiment performed in adult erGAP3-expressing transgenic Drosophila melanogaster *in vivo.* **(A)** The motor neurons were stimulated through the giant fiber system [34] with square 6 V/30 ms pulses at 0.25, 4 or 16 Hz, as shown. Images of F_{470} were captured every 100 ms (circles). **(B)** The first image (**F_{470}**) shows the green fluorescence of the thoracic muscles seen from the top. Calibration mark, 500 µM. The region of interest where the measurements were taken is also shown (white square). The rest of the images (**a-d**) were normalized as the ratio F/F_0 and coded in pseudocolor (scale at right). The exact moment at which each image was taken is shown at (A). **(C)** Superimposition of the responses to the three stimuli at an expanded time scale. The arrowheads denote two successive stimuli of the 0.25 Hz series. Note that the stimulation periods last for longer than the time shown and that the sampling period for imaging is of 1 image every 0.1 s.

Formatted: Wrap Around

Field Code Changed

Table 1. Low affinity Ca^{2+} indicators.

Name	Type	K_d (μM)	*n*	Dynamic range	λ(□□nm□)		Reference
					Ex.	Em.	
Synthetic probes							
Mag-Fura-2	Ex. ratiometric	53	1	1.7	350 385	510	[35]
Mag-Indo-2	Em. ratiometric	30	1	20	355	400 480	[36]
Rhod-5N	Intensiometric	320	1	50	551	575	[13]
CaGF	Intensiometric	60	1	2.5	488	530	[37]
GECIs							
YC4er	Em. ratiometric	0.08 700	1.5 0.87	1.5	440	485 535	[38]
D1ER	Em. ratiometric	0.8 60	1.18 1.63	1.5	440	485 535	[39]
D4cpv	Em. ratiometric	80	1.35	3.8	440	485 535	[40]
Split-YC7.3er	Em. ratiometric	130	1.4	2.6	440	485 535	[41]
CatchER	Intensiometric	180	0.94	1.5	490	510	[42]
Twitch	Em. ratiometric	253		4.4	432	475 527	[43]
G-CEPIA1er	Intensiometric	672	1.95	4.7	472	520	[11]
R-CEPIA1er	Intensiometric	565	1.7	8.8	562	641	[11]
GEM-	Em. ratiometric	558	1.37	21.7	377	466 520	[11]
D1ERCmR2	Em. ratiometric	220	0.5	1.1	480	560 510	[44]
GCaMPer	Intensiometric	238	0.93	2	490	540	[45]
LAR-GECO1	Intensiometric	24	1.3	10	559	647	[12]
erGAP1	Ex. ratiometric	16	1	4	405 470	550	[26]
erGAP3	Ex. ratiometric	489	0.9	3	405	550	[31]

cp, circularly permuted; n, Hill coefficient.

Formatted: Wrap Around

Field Code Changed

Fig. 1

A. AEQUORINS

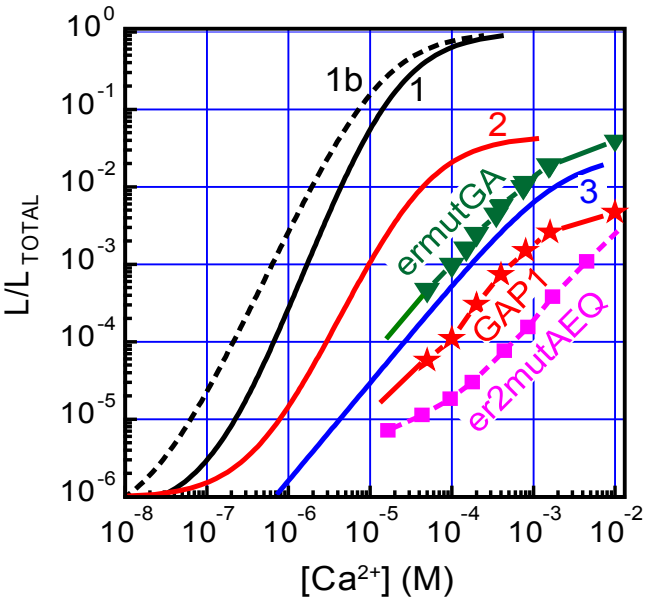

B. GAPs

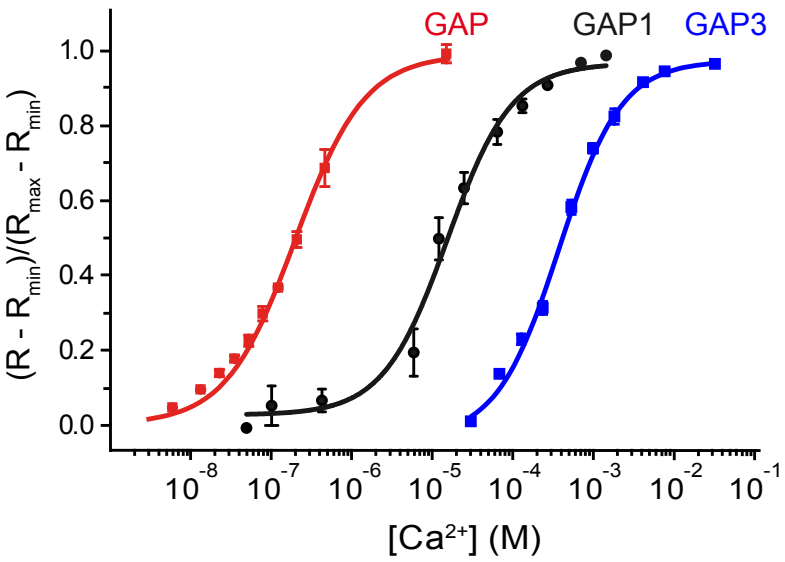

C. GAP model

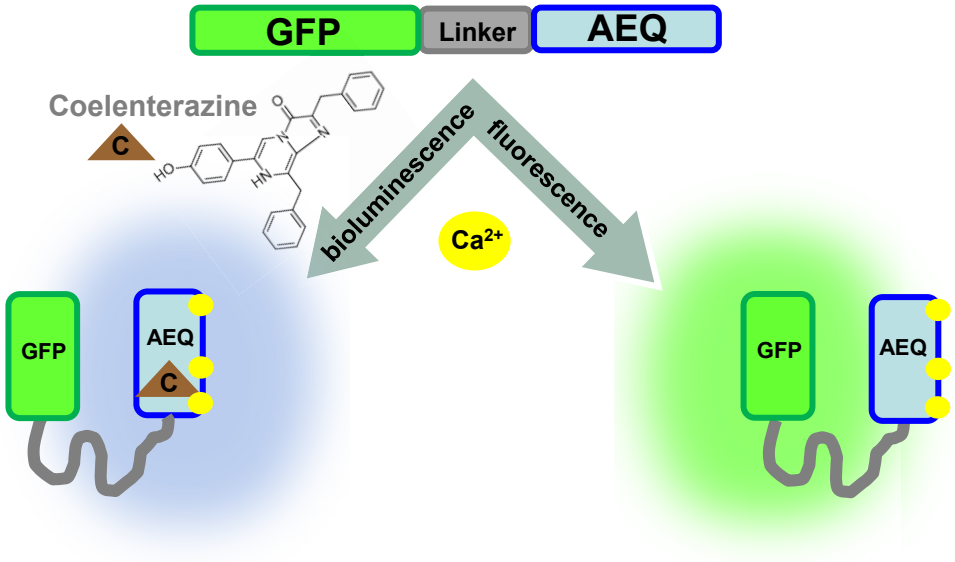

Fig. 2

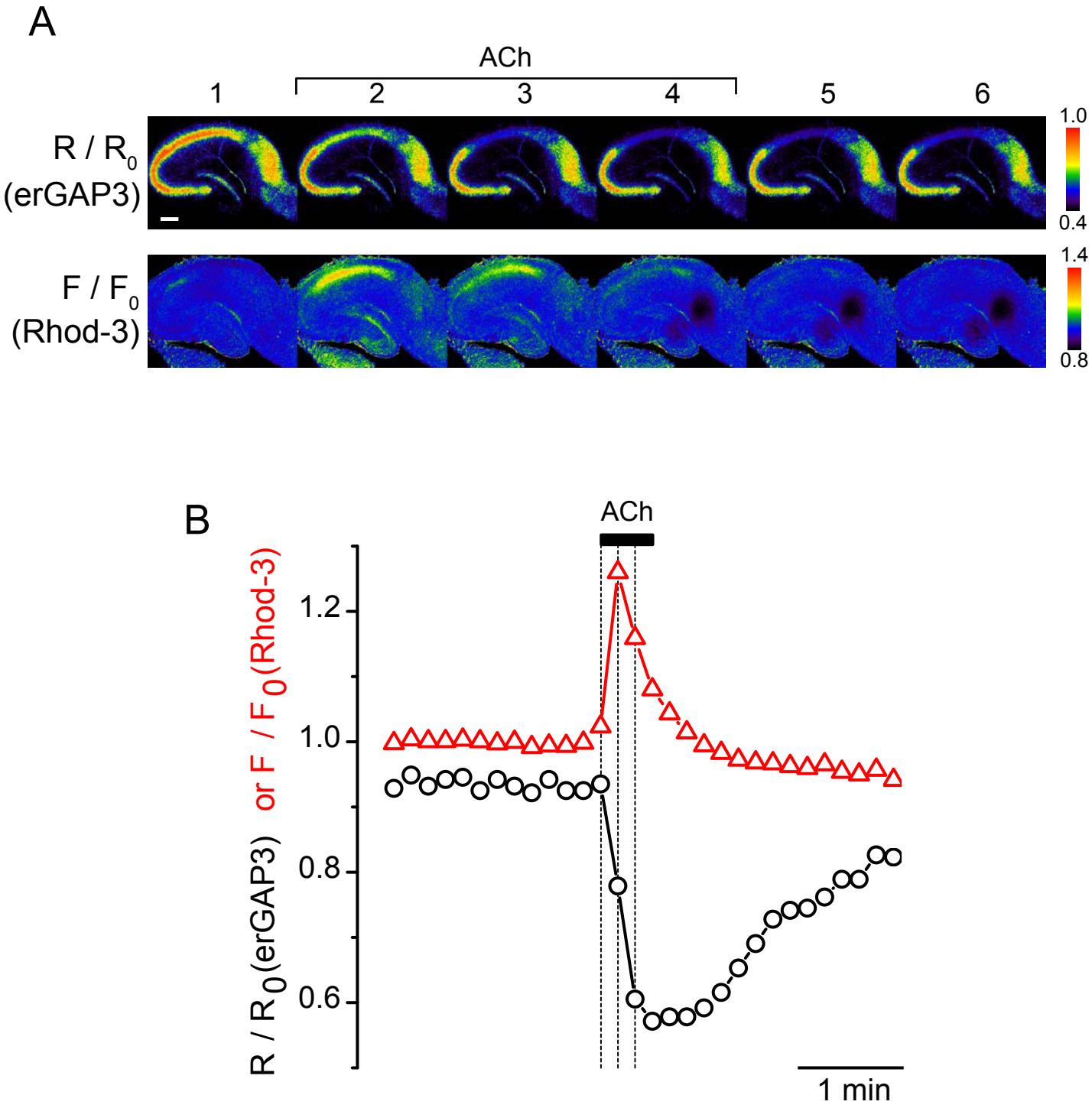
A
ACh
1
2
3
4
5
6
R / R0
(erGAP3)
1.0
0.4
F / F0
(Rhod-3)
1.4
0.8
B
ACh
R / R0(erGAP3) or F / F0(Rhod-3)
1.2
1.0
0.8
0.6
1 min

Fig. 3

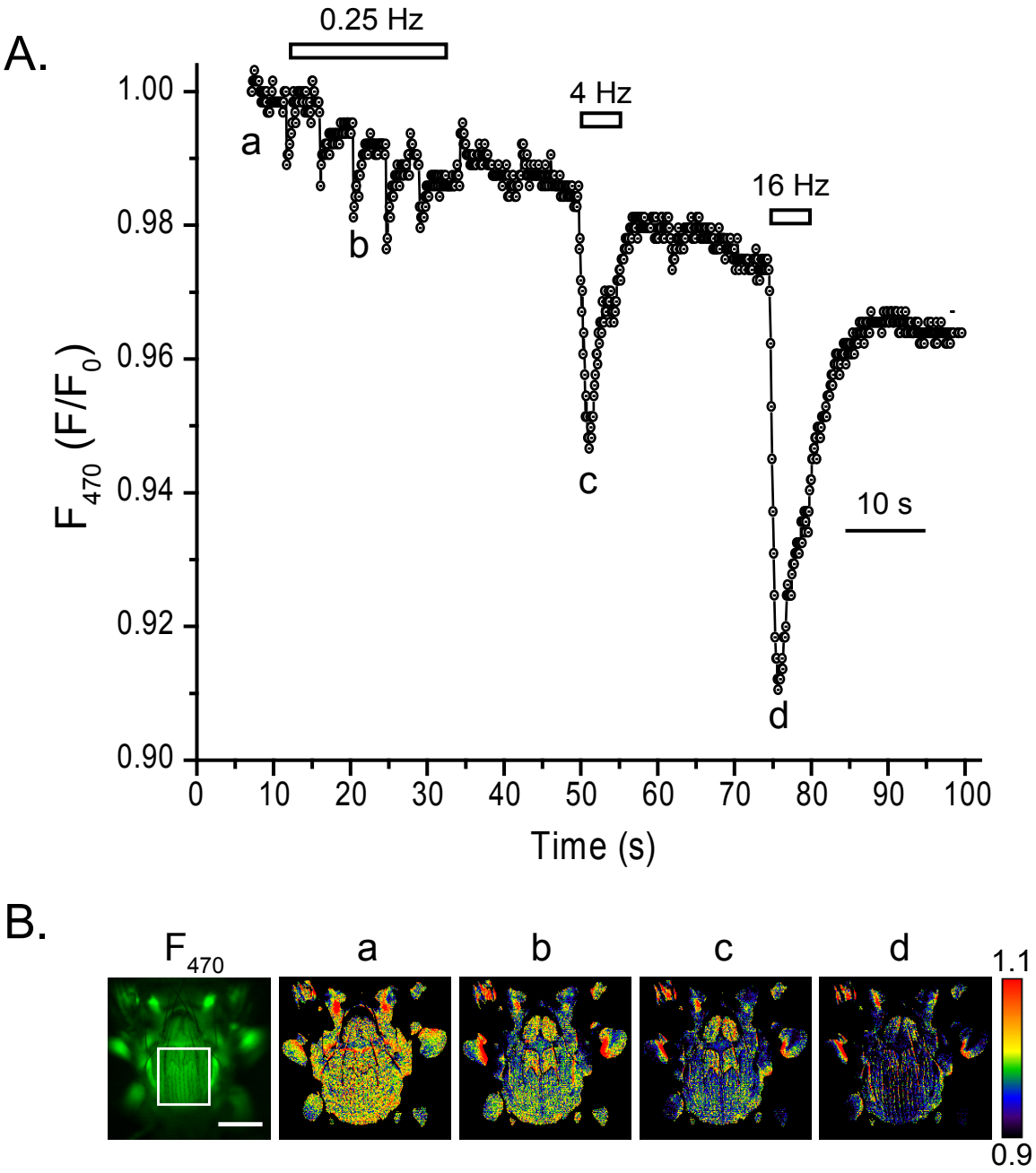
A.
0.25 Hz
4 Hz
16 Hz
a
b
c
d
10 s
1.00
0.98
0.96
0.94
0.92
0.90
F470 (F/F0)
0
10
20
30
40
50
60
70
80
90
100
Time (s)
B.
F470
a
b
c
d
1.1
0.9
C.
1 s
0.25 Hz
4 Hz
16 Hz
1.00
0.98
0.96
0.94
0.92
F470 (F/F0)